Supplement of Atmos. Meas. Tech., 12, 3365–3381, 2019
https://doi.org/10.5194/amt-12-3365-2019-supplement

Supplement of

The ICAD (iterative cavity-enhanced DOAS) method

Martin Horbanski et al.

Correspondence to: Martin Horbanski (martin.horbanski@iup.uni-heidelberg.de)

S1 ICAD Evaluation Including Aerosols

In this section we give a brief discussion of an ICAD evaluation with aerosols. The aerosol extinction, typically modeled with an Ångström exponent $\epsilon_{\text{aerosol}}(\vec{m}, \lambda) = m_1 \cdot \lambda^{m_2}$, has a relatively broadband wavelength dependency compared to trace gasses. However, due to the strong wavelength dependency of the path length $L_{\text{eff}}(\lambda)$, the effective reference spectrum

$$\vartheta_{\text{aerosol}}(\lambda) = \left(\bar{L}_{\text{eff}}(\lambda) \cdot \epsilon_{\text{aerosol}}(\vec{m}, \lambda)\right) \tag{1}$$

is sufficiently wavelength dependent. Therefore, it can be distinguished from other broadband variations, like instrumental intensity drifts e.g. of the LED, which do not take place in the cavity and therefore are not modulated with the path length curve. We used the simulations from section 1.3 plus aerosol extinction with a typical Ångström exponent of 1.7 and gaussian noise ($\sigma = 10^{-4}$). As an example we chose 10 ppbv NO_2 and a peak aerosol optical density of 20 %. Figure S2 shows the ICAD evaluation with aerosol absorption. Fit settings of config 1 (Table 1) are adapted, to get a good aerosol retrieval. A broader fit range 441 nm to 494 nm has to be chosen to include both wings of the aerosol fit reference (the shape of the aerosol extinction arises due to the mirror reflectivity), the DOAS polynomial is set to first order and the high pass binomial filter is removed. The ICAD evaluation correctly retrieves (9.97 ± 0.03) ppbv NO_2 which shows that the reduction of the light path by aerosol absorption is correctly accounted for by the correction factor $K(\lambda)$. This demonstrates that ICAD can in principle also be used in the presence of aerosol extinction. To derive optimal trace gas concentrations under real measurement conditions it is probably advisable to make a two stage fit. The first stage would a the broad fit range and reduced high pass filtering like in this example in order to retrieve the aerosol extinction. For an optimal trace gas fit, the second stage would include the aerosol extinction with fixed parameters and use the narrower fit range and high pass filtering, e.g. according to config 1 (Table 1). Further studies with aerosol application are beyond the scope of this manuscript.

S2 Comparison of Mobile Measurements to Air Quality Stations

The temporal variation of the NO_2 levels during the measurement cruise (from section 5.2) is further compared to the hourly NO_2 levels measured by the air quality stations operated by the state office for the environment, measurements and nature conservation of the federal state of Baden-Württemberg (LUBW) [1] (Fig. S5). The hourly averages of the ICAD NO_2 measurements are similar to the LUBW stations. This indicates that the large scale average of the NO_2 mixing ratio is well represented by the air quality network. However, on the local scale the ICAD time series shows a strong variability with peak values being almost four times higher than the hourly average. The peak levels of NO_2 regularly exceed 105 ppb, the hourly EU limit value. Such peak values are especially found in street canyons where ventilation is limited and at intersections of big roads where cars frequently accelerate from a standstill position. This hints, that there are areas where we have NO_2 levels are strongly underestimated by the average values from the monitoring stations, and therefore require a reassessment

---

[1] Data taken from the data and map service (UDO) of the LUBW. https://udo.lubw.baden-wuerttemberg.de Accessed 04-15-2018

of the air quality. However, to make a certain statement on the air quality measurement drove from this pilot study would need to be repeated over a longer time period and also would need to revisit the same points at different times of day to reduce systematic errors induced by traffic pattern and meteorology.

S3 Figures

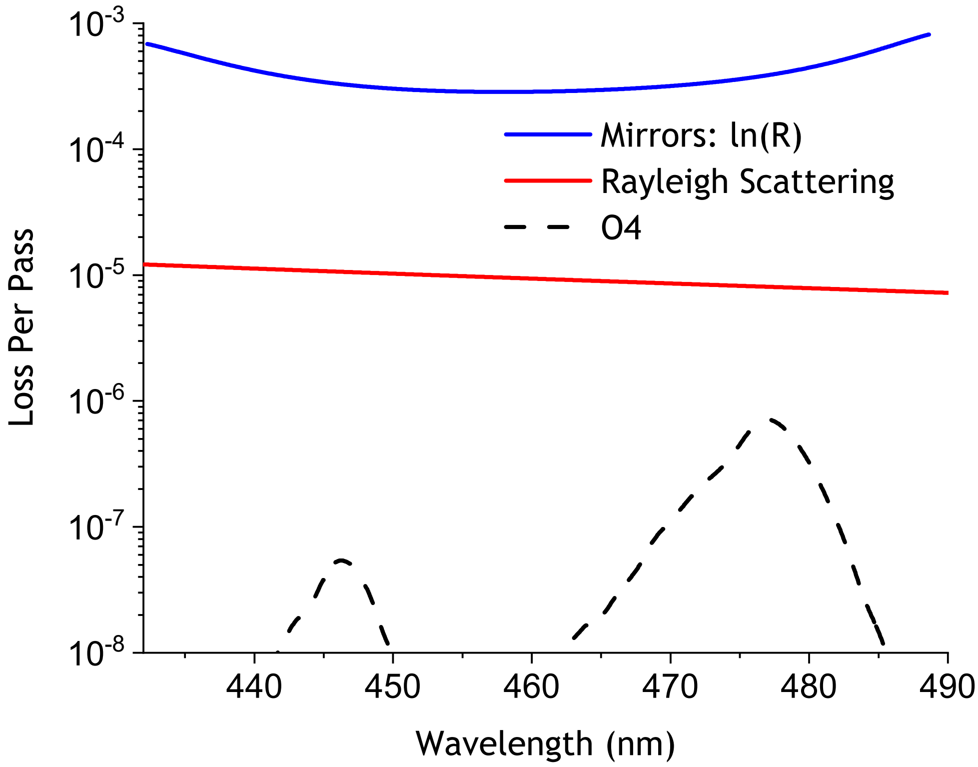

Figure S1 Loss per light pass in the resonator for the ICAD instrument config 1. The corresponding path length curve $\bar{L}_0(\lambda)$ is shown in Figure 2. It can be seen that the dominant contribution to the path length comes from the mirror reflectivity $R(\lambda)$. The contribution of Rayleigh scattering is almost two orders of magnitude lower and O4 absorption is almost negligible. Higher mirror reflectivities can be used to increase the path length as long as they contribute the dominant loss process.

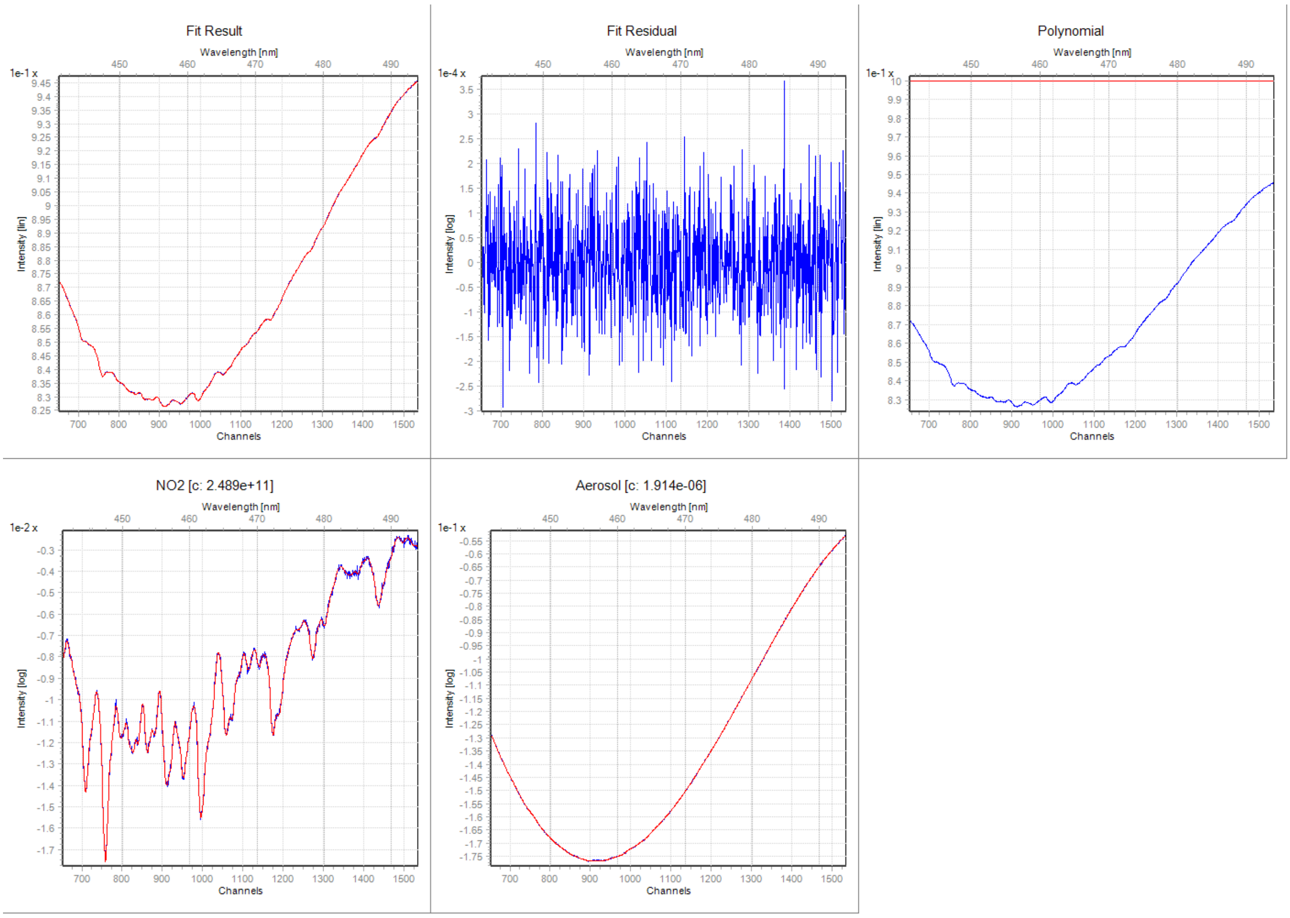

Figure S2 ICAD evaluation for a simulated spectrum with aerosol extinction. Simulations are based on section 1.3 with 10 ppbv NO_2 plus aerosol extinction with a typical Ångström exponent of 1.7 and a peak aerosol optical density of 20 % and gaussian noise ($\sigma = 10^{-4}$). Fit settings are based on config 1 (Table 1). A broader fit range 441 nm to 494 nm has to be chosen to include both wings of the aerosol fit reference, the DOAS polynomial is set to first order and the high pass binomial filter is removed. The ICAD evaluation correctly retrieves (9.97 ± 0.03) ppbv NO_2 which shows that the reduction of the light path by aerosol absorption is correctly accounted in the correction factor $K(\lambda)$.

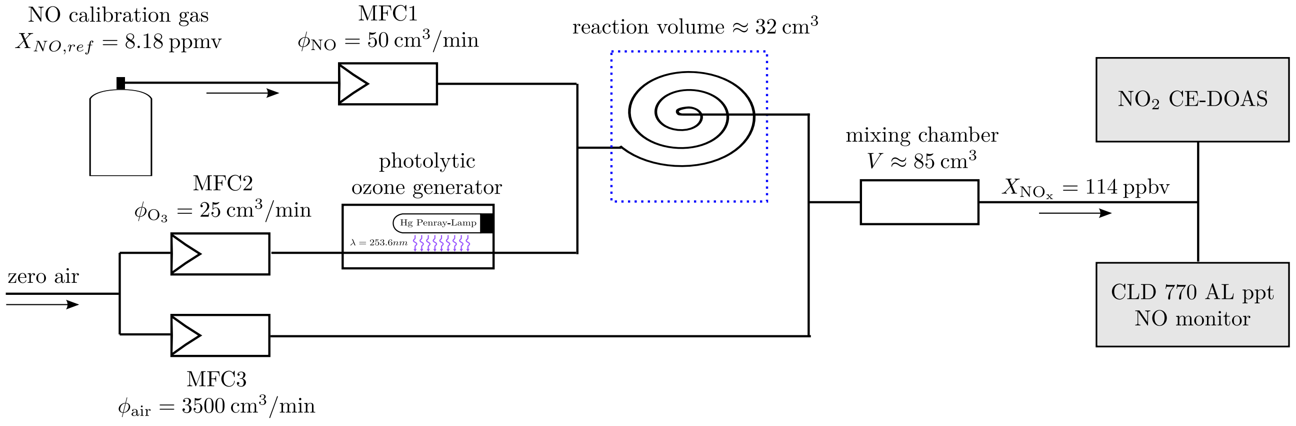

Figure S3 Measurement setup for the laboratory measurements. To produce NO_2, NO from a calibration gas cylinder is titrated with O_3, generated photolytically from zero air from a gas bottle. Two calibrated mass flow controllers (MFC1, MFC2) provide a constant gas flow. They are adjusted to ensure that the gas phase titration is completed to at least 99% after one third of the residence time in the reaction volume. After the titration the gas mixture is further diluted with zero air to achieve a $\mathrm{NO_x}$ mixing ratio of 114 ppbv. During the measurement all gas flows are kept constant. To produce different NO_2 mixing ratios the O_3 concentration is adjusted through the electrical current of the UV-light source. Simultaneously to the NO_2 ICAD measurements, the NO mixing ratio in the sample gas is measured by a calibrated NO chemiluminescence detector (Eco Systems, CLD 770 Al ppt). This allows to calculate the exact NO_2 mixing ratio from the comparison with a measurement at deactivated ozone generator as the total $\mathrm{NO_x}$ mixing ratio is constant ($X_{\mathrm{NO_2}} = X_{\mathrm{NO}_x} - X_{\mathrm{NO}}$).

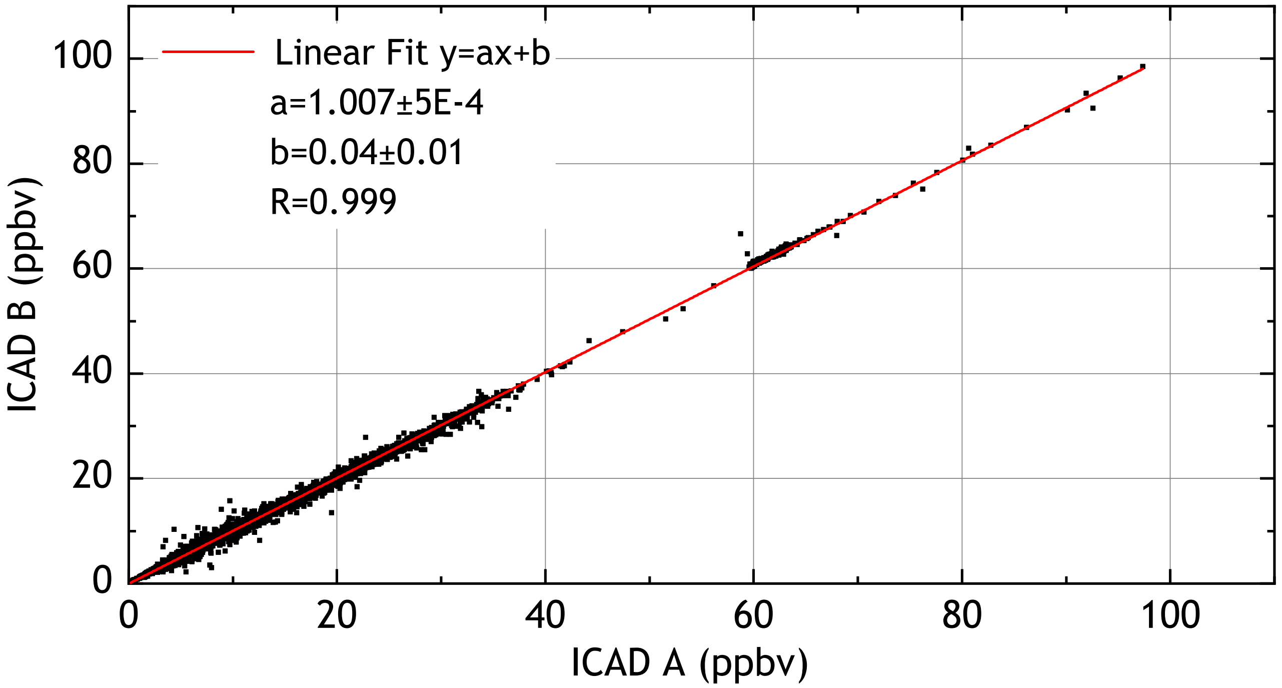

Figure S4 Correlation plot between ICAD NO_2 instruments A and B. The NO_2 concentrations show a very good linear correlation (Pearson's R of 0.999) with a slope of $1.007 \pm 5 \cdot 10^{-4}$ and a very low offset of (0.04 ± 0.01) ppbv.

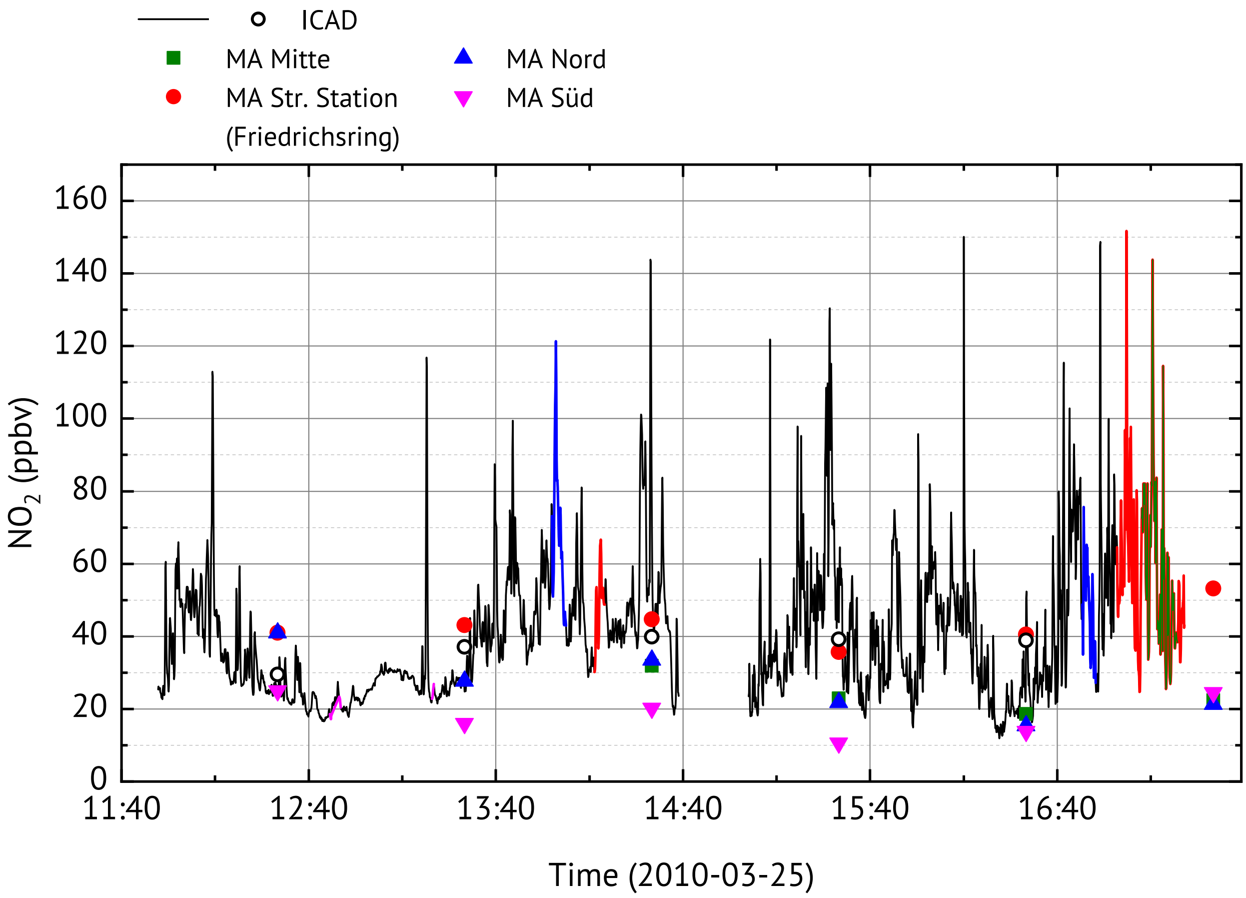

Figure S5 NO$_2$ time series for the automobile measurements (instrument configuration 1). The line graph shows the ICAD measurements at full time resolution. Additionally the hourly averages from the ICAD and four air quality stations are shown for comparison. The line graph has the colour of an air quality station at time intervals where the car is closer than 1.5 km to the station.